

Spin Manipulation in Graphene by Chemically-Induced Sublattice Pseudospin Polarization

Dinh Van Tuan¹ and Stephan Roche^{1,2}

¹*Catalan Institute of Nanoscience and Nanotechnology (ICN2),
CSIC and The Barcelona Institute of Science and Technology,
Campus UAB, Bellaterra, 08193 Barcelona, Spain*

²*ICREA, Institució Catalana de Recerca i Estudis Avançats, 08070 Barcelona, Spain**

(Dated: March 3, 2016)

Spin manipulation is one of the most critical challenges to realize spin-based logic devices and spintronic circuits. Graphene has been heralded as an ideal material to achieve spin manipulation but so far new paradigms and demonstrators are limited. Here we show that certain impurities such as fluorine ad-atoms, which locally break sublattice symmetry without the formation of strong magnetic moment, could result in a remarkable variability of spin transport characteristics. The impurity resonance level is found to be associated with a long range sublattice pseudospin polarization, which by locally decoupling spin and pseudospin dynamics, provokes a huge spin lifetime electron-hole asymmetry. In the dilute impurity limit, spin lifetimes could be tuned electrostatically from hundred picoseconds to several nanoseconds, providing a protocol to chemically engineer an unprecedented spin device functionality.

PACS numbers: 72.80.Vp, 71.70.Ej, 75.76.+j

Introduction. The possibility to fine tune the electronic, charge and spin transport properties of graphene using chemical functionalization^{1–4}, irradiation (defect formation)⁵, electric fields⁶ or antidot fabrication⁷ has become an exciting field of research with almost endless possibilities. In particular, chemical treatments such as ozonisation, hydrogenation, or fluorination, introducing a variable density of surface ad-atoms from typically 0.001% to few percent, have demonstrated a large spectrum of accessible physical states from anomalous transport to highly insulating behavior of chemically reactive graphene derivatives^{8–12}. On the other hand, graphene exhibits long room temperature spin lifetime and rich surface chemistry opportunities which could be harnessed for the development of all-spin logic technologies^{13–20}. As a matter of illustration, the use of chemical fluorination of graphene bilayer has been shown to yield very high spin injection efficiency (above 60%), owing to improved interface spin filtering²¹.

Spin lifetime is an essential quantity that fixes the upper time and length scales on which spin devices can operate, so that knowing its value and variability are prerequisite to realizing graphene spintronic technologies. The sources of spin relaxation turn out to be diversified in graphene, and extrinsic disorder driven by ad-atom impurities can significantly enhanced spin-orbit interaction around defects¹, or create local magnetism²²; both effects usually reducing spin lifetimes, even in the dilute limit^{23–31}.

The nature of spin relaxation in graphene has been initially discussed either in terms of Elliot-Yafet²⁴ or Dyakonov-Perel³² mechanisms, depending on the scaling of spin lifetime with defect density. However recently, a novel spin relaxation mechanism in non-magnetic graphene samples has been connected to the unique spin-pseudospin entanglement occurring near the Dirac

point, pointing towards revisiting the role of sublattice pseudospin³³.

Sublattice pseudospin is an additional quantum degree of freedom, mathematically very similar to spin and unique to graphene sublattice degeneracy¹. In absence of spin-orbit coupling, the low-energy electronic states write $\Psi_{\vec{k}}(\vec{r}) \sim (\psi_A(1,0)^T + \psi_B(0,1)^T) \times e^{i\vec{k}\vec{r}}$, where $(1,0)^T$ and $(0,1)^T$ define up and down-pseudospin states, while ψ_A (resp. ψ_B) give the wavefunction weight restricted to A (resp. B) sublattice sites^{1,34}. In addition to sublattice pseudospin, valley isospin (for the two K-points in the reciprocal space) also shows up in the electronic wavefunctions, and harnessing these degrees of freedom is the target of "Valleytronics and Pseudospintronics"^{35,36}. The complex interplay between sublattice pseudospin and valley isospin is currently the source of innovative device proposals such as valley or pseudospin filtering and switches^{6,37–42}.

In presence of a Rashba spin-orbit coupling (SOC) field either generated by a substrate-induced electric field or a weak density of metal ad-atoms (gold, nickel), spin and pseudospin become strongly coupled at the Dirac point where the eigenstates take the form $\Psi_{\vec{k}=\vec{K}} \sim (1,0)^T \times |\downarrow\rangle \pm i(0,1)^T \times |\uparrow\rangle$, where $|\downarrow\rangle$ and $|\uparrow\rangle$ denote the spin state^{33,43}. Such spin-pseudospin locking drives to an entangled dynamics of spin and pseudospin resulting in fast spin dephasing, even when approaching the ballistic limit³³, with increasing spin lifetimes away from the Dirac point, as observed experimentally⁴⁴. This phenomenon suggests ways to engineer spin manipulation based on controlling the pseudospin degree of freedom (or vice versa), which would help in the development of spin logics^{16,19,20}.

In this Letter, we reveal that chemical functionalization of graphene with certain types of ad-atoms such as

fluorine, by breaking the sublattice symmetry and by inducing a SOC without the formation of strong magnetic moment, provide an enabling technique to monitor spin transport properties in a remarkable way for spintronic applications. The fluorine ad-atoms indeed produce hole impurity levels which exhibit a long range spatial sublattice pseudospin polarization (SPP), which counteracts the homogeneous Rashba SOC field at the origin of the intrinsic spin precession and relaxation in the otherwise fluorine free samples⁴⁵. As a result, spin and pseudospin dynamics are not anymore coupled at the impurity resonances, which lead to the possibility to electrostatically tune spin lifetime by up to one order of magnitude (for instance under electrostatic gating). This is a theoretical opportunity for designing a new kind of spin transistor effect based on a gate-controlled spin transport length. Calculations are performed using a realistic tight-binding model elaborated from ab-initio calculations, whereas the spin dynamics is computed through the time-evolution of the expectation value of the spin operator projected on a real space basis set.

Tight-binding description of fluorinated graphene. The description of fluorine ad-atom on graphene is achieved using a tight-binding model elaborated from ab-initio simulations⁴⁶. The Hamiltonian for the system involves two parts:

$$\mathcal{H} = \mathcal{H}_G + \mathcal{H}_{FG} \quad (1)$$

The first part describes the graphene in a homogeneous SOC field induced by the substrate or gate voltage

$$\begin{aligned} \mathcal{H}_G = & -\gamma_0 \sum_{\langle ij \rangle} c_i^\dagger c_j + \frac{2i}{9} \lambda_I \sum_{\langle\langle ij \rangle\rangle} c_i^\dagger \vec{s} \cdot (\vec{d}_{kj} \times \vec{d}_{ik}) c_j \\ & + \frac{2i}{3} \lambda_R \sum_{\langle ij \rangle} c_i^\dagger \vec{z} \cdot (\vec{s} \times \vec{d}_{ij}) c_j \end{aligned} \quad (2)$$

where γ_0 is the usual π -orbital hopping term between nearest-neighbors, $\lambda_I = 12 \mu\text{eV}$ is commonly value used for the intrinsic SOC of graphene⁴⁷ while the Rashba SOC λ_R is an electric field-dependent quantity. In this study we take $\lambda_R = 37.4 \mu\text{eV}$ taken from an extended *sp*-band tight-binding model⁴⁸ for graphene under the influence of an electric field of 0.1 V/\AA , induced by the substrate or the gate voltage.

The second part \mathcal{H}_{FG} describes the influences of fluorine on graphene

$$\begin{aligned} \hat{\mathcal{H}}_{FG} = & \epsilon_F \sum_m F_m^\dagger F_m + T \sum_{\langle mi \rangle} [F_m^\dagger A_i + h.c.] \\ & + \frac{2i}{9} \Lambda_I^B \sum_{\langle\langle ij \rangle\rangle} B_i^\dagger \vec{s} \cdot (\vec{d}_{kj} \times \vec{d}_{ik}) B_j \\ & + \frac{2i}{3} \Lambda_R \sum_{\langle ij \rangle} [A_i^\dagger \vec{z} \cdot (\vec{s} \times \vec{d}_{ij}) B_j + h.c.] \\ & + \frac{2i}{3} \Lambda_{PIA} \sum_{\langle\langle ij \rangle\rangle} B_i^\dagger \vec{z} \cdot (\vec{s} \times \vec{d}_{ij}) B_j \end{aligned} \quad (3)$$

with all the parameters $\epsilon_F = -2.2 \text{ eV}$, $T = 5.5 \text{ eV}$, $\Lambda_I^B = 3.3 \text{ meV}$, $\Lambda_R = 11.2 \text{ meV}$, and $\Lambda_{PIA}^B = 7.3 \text{ meV}$ are derived from ab-initio simulations⁴⁶. The operator F (F^\dagger) annihilates (creates) an electron in the atomic p_z orbital on fluorine F. A and B (A^\dagger and B^\dagger) denote the annihilation (creation) operators for p_z orbital on fluorinated carbons and their nearest neighbors, respectively. The first term in above Hamiltonian is the on-site energy term on the fluorine ad-atoms and the second term is the hopping term between fluorine ad-atoms F and fluorinated carbon $A \equiv C_F$. The third and the fourth terms which are similar to the SOC terms in Eq.(2) simulate the local intrinsic and Rashba SOC induced by the absorption of fluorine on graphene. Finally the last term, the new SOC term, coming from the pseudospin inversion asymmetry (PIA) mediates the spin-flip hopping between two second nearest neighbors B_i . It is worth mentioning that we are using the π -orbital tight binding model which is different from a recent paper on the electronic structures and optical properties of fluorinated graphene in which the multi-orbital tight-binding was employed⁴⁹.

Spin dynamics methodology. The spin dynamics of electron in fluorinated graphene is investigated using the time-dependent evolution of the spin polarization of propagating wavepackets³³. Simulations of samples of μm^2 size are performed, containing hundred millions of carbon atoms ($N \sim 10^8$). The time-evolution of the spin polarization is computed through

$$\vec{P}(E, t) = \frac{\langle \Psi(t) | \vec{s} \delta(E - \mathcal{H}) + \delta(E - \mathcal{H}) \vec{s} | \Psi(t) \rangle}{2 \langle \Psi(t) | \delta(E - \mathcal{H}) | \Psi(t) \rangle} \quad (4)$$

where \vec{s} are the spin Pauli matrices and $\delta(E - \mathcal{H})$ is the spectral measure operator. The time evolution of electronic wavepackets $|\Psi(t)\rangle$ is obtained by solving the Schrödinger equation^{50,51}, starting from random-phase states $|\Psi(t=0)\rangle = |\varphi_{\text{RP}}\rangle$ with an initial out-of-plane (z direction) or in-plane polarization (x, y direction). The random phase states can be generally expressed as $|\varphi_{\text{RP}}\rangle = \frac{1}{\sqrt{N}} \sum_{j=1}^N \begin{pmatrix} \cos(\theta_j/2) \\ e^{i\Phi_j} \sin(\theta_j/2) \end{pmatrix} e^{2i\pi\alpha_j} |j\rangle$, where (Φ_j, θ_j) gives the spin orientation of orbital $|j\rangle$ in the spherical coordinate, whereas α_j is a random number in the $[0, 1]$ interval³³. An energy broadening parameter η is introduced for expanding $\delta(E - \mathcal{H})$ through a continued fraction expansion of the Green's function^{50,51}. An average over few tens of random phases states is usually sufficient to converge the expectation values. This method has been previously used to investigate spin relaxation in gold-decorated graphene³³, hydrogenated graphene²⁶ and recently, SOC coupled graphene under the effect of electron-hole puddles⁴⁵.

Impurity resonance and sublattice pseudospin polarization. Electronic calculations show that unlike hydrogen, the fluorine adatom is a broad scatterer⁴⁶. The density of states (DOS) of a 40×40 supercell (about 0.03%) exhibits a resonant peak at about 260 meV⁴⁶ below the Dirac point. Fig. 1 shows the local density of state (LDOS) on the sites close to the fluorinated carbon C_F

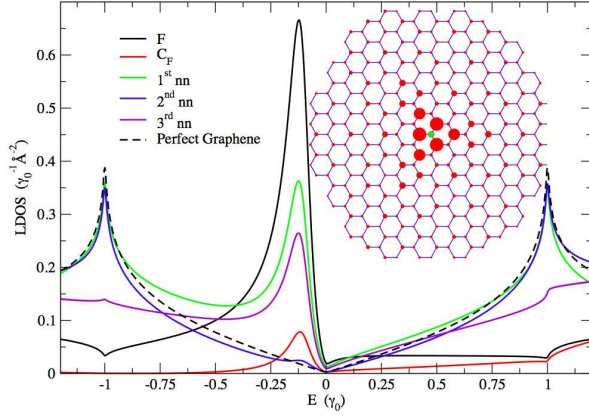


FIG. 1. Local density of state (LDOS, solid lines) around the fluorinated carbon C_F in the comparison with the pristine graphene one (dashed line). Inset: SPP around the fluorinated carbon (marked by the green circle). The radii of the circle is proportional to the LDOS, the state is projected at the resonant energy $E_R = -0.125\gamma_0$.

using the tight-binding model for \mathcal{H} (Eq.(1)). All the LDOSs present a strong electron-hole asymmetry with broad peaks at about $E_R = -0.125\gamma_0 = -325$ meV which are evidences of fluorine-induced resonant effect. More interestingly, the height of resonant peaks discloses a sublattice asymmetry with less state occupancy on the sublattice related to the fluorinated carbon C_F . This is the signature of a SPP which is present in graphene when the A-B symmetry is broken such as in the case of hydrogenated, nitrogen-doped graphene or graphene with vacancies. Fluorine ad-atoms induce a long range pseudospin-polarized region. Fig. 1 (inset) shows the LDOS at the resonant energy E_R (represented by the radius of circles) on more than 300 atoms around the fluorinated carbon (marked by the green dot). At the edge of this area one can still see the difference between LDOSs on two different sublattices. Here we will show that the SPP has a direct impact on spin lifetime in fluorinated graphene.

Strong electron-hole asymmetry of the spin lifetime.

We compute the expectation value of the out-of-plane spin component $P_z(E, t) = P_\perp(E, t)$ and the in-plane spin component $P_x(E, t) = P_\parallel(E, t)$ of spin polarization in fluorinated graphene using Eq.(4). Fig. 2c (inset) shows the evolution of spin polarization $P_z(t)$ at the Dirac point (black and green solid lines) and at the resonant energies E_R (red and blue solid lines) for 0.01% and 0.02% of fluorine on graphene. There are two interesting features of the spin signals. The first one is the remarkably slow decay of the time-evolution of the spin polarization at the resonance ($E = E_R$) compared to that occurring at the Dirac point. The second characteristic is the enhancement of spin polarization when increasing the percentage of fluorine (see illustration in Fig. 2a and

Fig. 2b).

Such remarkable features are further manifested in the spin lifetime τ_s (Fig. 2c, main frame), which are extracted from the spin polarization by fitting the obtained data with an exponential decay $P_{x,z}(t) = P_{x,z}(t_0)e^{-(t-t_0)/\tau_s^{\parallel,\perp}}$ (dashed lines in the inset of Fig. 2c). This fitting is performed starting from the time $t_0 = 30$ ps to avoid the initially transient fast decay which is usually observed for strong disorder, especially at DP²⁶. The spin lifetime exhibits a strong electron-hole asymmetry with huge increase of spin lifetime with a maximum close to but not exactly at the resonant energy (about one order of magnitude compared to one in the electron side).

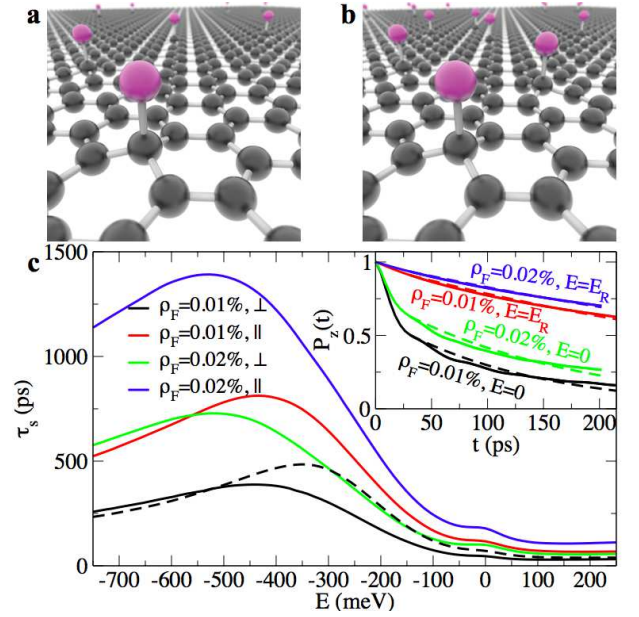


FIG. 2. (a) and (b) show ball-and-stick models for fluorine functionalized graphene for two different densities. (c) spin relaxation time τ_s for in-plane \parallel and out-of-plane \perp spin components for 0.01% and 0.02% of fluorine on graphene (dashed line gives τ_s^\perp for 0.01% fluorine, neglecting the SOC term). Inset: spin polarization evolution at the Dirac point and at resonant energy E_R for 0.01% and 0.02% of fluorine on graphene.

The energy of this maximum is shifted to the hole side compared to the resonant energy E_R and this energy shift increases with the fluorine concentration. This shift is attributed to the SOC effects caused by fluorine ad-atoms. Indeed, turning off the SOC induced by fluorine leads to the spin lifetime (dashed line) with the peak exactly at resonant energy E_R . More remarkably, the increase of fluorine percentage leads to an enhancement of τ_s (Fig. 2c). This is counterintuitive because fluorine was predicted to induce a giant SOC in graphene which should lead to a decrease of spin lifetime with fluorine density ρ_F ⁴⁶. Actually, the SOC induced by fluorine does not play a major role here. Indeed, in absence of SOC induced by fluorine ($\Lambda_I^B = \Lambda_R = \Lambda_{PIA} = 0$), τ_s shows

similar energy dependence (see dashed line in Fig. 2c for τ_s^\perp and 0.01% fluorine atoms neglecting their SOC contribution).

Dyakonov-Perel mechanism. Fluorine ad-atoms also induce momentum scattering which yield randomization of the spin precession. This usually leads to a Dyakonov-Perel relaxation mechanism in which the spin lifetime τ_s is inversely proportional the momentum relaxation time τ_p , i.e. $\tau_s^\parallel = 2\tau_s^\perp = \hbar^2/(2\lambda_R^2\tau_p)^{32,52-54}$. This scaling can be clearly observed in Fig. 2c where τ_s upscales with the fluorine density ρ_F almost linearly as expected from a Fermi golden rule argument. To further confirm the mechanism at play, the momentum relaxation time τ_p is computed numerically using a real-space order-N approach⁵¹.

Fig. 3a shows the energy dependence of τ_p for 0.02% of fluorine on graphene with a minimum close to E_R , pinpointing the resonance induced by fluorine (identified by the peak in the LDOS of atoms in the distance of twice carbon bond length from C_F , see red dashed line). To further confirm the relaxation mechanism, we compute the product of $\tau_s\tau_p$ (see Fig. 3b). The obtained numerical data (black solid line) close to the resonance are fairly consistent with a Dyakonov-Perel mechanism (red dashed line) up to a factor $\alpha \in [0.6; 1.4]$ ($\tau_s^\parallel\tau_p = \frac{\alpha\hbar^2}{2\lambda_R^2}$). A final evidence is given by the spin lifetime anisotropy of τ_s obtained in Fig. 3c. Indeed, the ratio of in-plane and out-of-plane spin lifetimes $\tau_s^\parallel/\tau_s^\perp \sim 2$ (within 10% error), well agrees with analytical calculations performed in model systems⁵⁴. Some deviation is observed close to the Dirac point, where the spin-pseudospin entanglement effects are maximized.

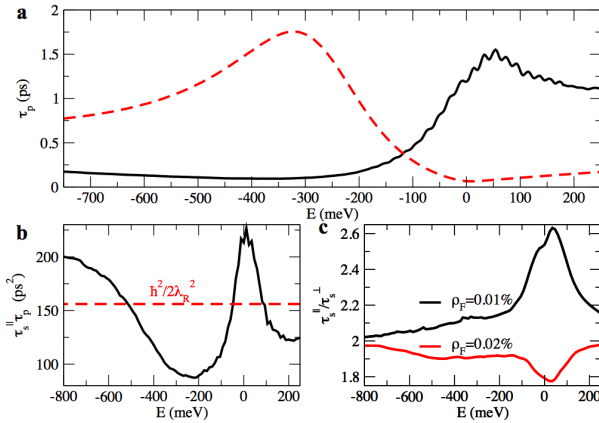


FIG. 3. (a) Energy dependence of the momentum relaxation time τ_p for 0.02% of fluorine on graphene. (b) Numerical product of $\tau_s^\parallel\tau_p$ compared with the analytical value (dashed line) from ref.³². (c) The ratio of in-plane and out-of-plane spin relaxation times for 0.01% and 0.02% of fluorine on graphene.

Discussion. The enhancement and the energy-

dependence of τ_s is a direct consequence of defect-induced sublattice pseudospin polarization (illustrated in Fig. 1, inset). In supported ultraclean graphene, the Rashba SOC λ_R induced by the substrate or the gate voltage dictates the spin dephasing of propagating charges, as shown experimentally⁴⁴. It is worth mentioning that the spin lifetime caused by this background Rashba SOC is totally electron-hole symmetric⁴⁵. On the hole side, the induced SPP around fluorine defects locally suppress the Rashba SOC and consequently enhance spin lifetime up to the range of nanoseconds whereas τ_s is more strongly reduced on the electron side, with $\tau_s \sim 100$ ps. This phenomenon can be qualitatively understood using both the continuum and tight-binding models. In the continuum model, the Hamiltonian \mathcal{H}_G (Eq.(2)), including spin-orbit interaction, can be approximated as $h_G(\vec{k}) = \hbar v_F(\eta\sigma_x k_x + \sigma_y k_y) + \lambda_R(\eta\sigma_x s_y - \sigma_y s_x) + \lambda_I\eta\sigma_z s_z$, where σ and s are Pauli matrices representing the sublattice pseudospin and spin degrees of freedom respectively, while $\eta = 1(-1)$ corresponds to the K (K') valley (here intervalley coupling is neglected in the discussion). The magnitude of the Rashba magnetic field is proportional to the in-plane component of pseudospin $(\sigma_x, \sigma_y)^{33}$ which is reduced by approaching the area around fluorine due to the formation of SPP. The reduction of local effective Rashba magnetic field entails the enhancement of spin lifetimes which is maximum close to the resonant energy E_R where the SPP is maximum. In the tight-binding model, the peculiar sublattice occupancy of impurity states gives rise to an increase of the next-nearest-neighbor hopping probability (intrinsic SOC) and a decrease of the nearest-neighbor hopping probability (Rashba SOC), which being the main factor for spin relaxation, also explains the spin lifetime enhancement.

One notes that SPP is not unique to fluorine adsorption in the weak density limit, but can be also generated by nitrogen substitutions⁵⁵, grafted molecules⁵⁶, hydrogen ad-atoms or any other effect breaking A-B sublattice symmetry. However the unveiled phenomenon of electron-hole spin transport asymmetry should be maximized in absence of magnetic moments, which disfavor long spin propagation^{25,26}. Besides, in contrast to the Elliot-Yafet mechanism predicted for magnetic impurities^{25,26,30}, ad-atoms such as fluorine are here shown to entail a Dyakonov-Perel mechanism, in agreement with many experiments on functionalized graphene^{57,58}. We note that the considered dilute fluorine limit is accessible experimentally^{59,60}, and that chemical bonding of fluorine ad-atoms is theoretically tunable with electric field⁶¹⁻⁶³, a fact which could help controlling the level of adsorption and the possibility to switch on and off the spin transport asymmetry generated by impurities. Finally we observe that spin dynamics could be a smoking gun for unveiling new quantum phase transition resulting from the competition between different ground states (such as those characterized by spin-degenerate and magnetic bound states⁶⁴), or to scrutinize the origin of the saturation of coherence times in

weak localization measurements⁶⁵.

Acknowledgements. This work has received funding from the European Union Seventh Framework Programme under grant agreement 604391 Graphene Flagship. S.R. acknowledges the Spanish Ministry of Econ-

omy and Competitiveness for funding (MAT2012-33911), the Secretaria de Universidades e Investigacion del Departamento de Economia y Conocimiento de la Generalidad de Cataluña and the Severo Ochoa Program (MINECO SEV-2013-0295).

* stephan.roche@icn.cat

- ¹ A. H. Castro Neto, F. Guinea, N. M. R. Peres, K. S. Novoselov, and A. K. Geim, *Rev. Mod. Phys.* **81**, 109 (2009).
- ² A. Krasheninnikov and F. Banhart, *Nature Materials* **6**, 723 (2007).
- ³ K. P. Loh, Q. Bao, P. K. Ang, and J. Yang, *J. Mater. Chem.* **20**, 2277 (2010).
- ⁴ M. F. Craciun, I. Khrapach, M. D. Barnes, and S. Russo, *Journal of Physics: Condensed Matter* **25**, 423201 (2013).
- ⁵ R. R. Nair, M. Sepioni, I.-L. Tsai, O. Lehtinen, J. Keinonen, A. Krasheninnikov, T. Thomson, A. K. Geim, and I. V. Grigorieva, *Nature Physics* **6**, 199 (2012).
- ⁶ Y. Son, L. Cohen, and S. Louie, *Nature* **444**, 347 (2006).
- ⁷ T. G. Pedersen, C. Flindt, J. Pedersen, N. A. Mortensen, A.-P. Jauho, and K. Pedersen, *Phys. Rev. Lett.* **100**, 136804 (2008).
- ⁸ D. Elias, R. Nair, T. Mohiuddin, S. Morozov, P. Blake, M. Halsall, A. Ferrari, D. Boukhvalov, M. Katsnelson, A. Geim, and K. Novoselov, *Science* **323**, 610 (2009).
- ⁹ F. Withers, M. Dubois, and A. K. Savchenko, *Phys. Rev. B* **82**, 073403 (2010).
- ¹⁰ J. Moser, H. Tao, S. Roche, F. Alzina, C. M. Sotomayor Torres, and A. Bachtold, *Phys. Rev. B* **81**, 205445 (2010).
- ¹¹ S.-H. Cheng, K. Zou, F. Okino, H. R. Gutierrez, A. Gupta, N. Shen, P. C. Eklund, J. O. Sofo, and J. Zhu, *Phys. Rev. B* **81**, 205435 (2010).
- ¹² J. T. Robinson, J. S. Burgess, C. E. Junkermeier, S. C. Badescu, T. L. Reinecke, F. K. Perkins, M. K. Zalalutdinov, J. W. Baldwin, J. C. Culbertson, P. E. Sheehan, and E. S. Snow, *Nano Letters* **10**, 3001 (2010).
- ¹³ N. Tombros, C. Jozsa, M. Popinciuc, H. Jonkman, and B. Van Wees, *Nature* **448**, 571 (2007).
- ¹⁴ B. Dlubak, M.-B. Martin, C. Deranlot, B. Servet, S. Xavier, R. Mattana, M. Sprinkle, C. Berger, W. de Heer, F. Petroff, A. Anane, P. Seneor, and A. Fert, *Nature Physics* **8**, 557 (2012).
- ¹⁵ P. Seneor, B. Dlubak, M. Martin, A. Anane, H. Jaffres, and A. Fert, *MRS Bulletin* **37**, 1245 (2012).
- ¹⁶ H. Dery, H. Wu, B. Ciftcioglu, M. Huang, S. Yang, R. Kawakami, J. Shi, I. Krivorotov, I. Zutic, and L. Sham, *IEEE Trans. Electron Devices* **59**, 259262 (2012).
- ¹⁷ M. B. Lundberg, R. Yang, J. Renard, and J. A. Folk, *Phys. Rev. Lett.* **110**, 156601 (2013).
- ¹⁸ M. Venkata Kamalakar, C. Groenveld, A. Dankert, and S. Dash, *Nature Comm.* **6**, 6766 (2015).
- ¹⁹ R. K. Kawakami, *2D Materials* **2**, 034001 (2015).
- ²⁰ S. Roche, J. Akerman, B. Beschoten, J.-C. Charlier, M. Chshiev, S. P. Dash, B. Dlubak, J. Fabian, A. Fert, M. Guimares, F. Guinea, I. Grigorieva, C. Schenberger, P. Seneor, C. Stampfer, S. O. Valenzuela, X. Waintal, and B. van Wees, *2D Materials* **2**, 030202 (2015).
- ²¹ A. Friedman, O. vant Erve, C. Li, J. Robinson, and B. Jonker, *Nature Comm.* **5**, 3161 (2014).
- ²² O. V. Yazyev, *Phys. Rev. Lett.* **101**, 037203 (2008).
- ²³ D. Huertas-Hernando, F. Guinea, and A. Brataas, *Phys. Rev. Lett.* **103**, 146801 (2009).
- ²⁴ H. Ochoa, A. H. Castro Neto, and F. Guinea, *Phys. Rev. Lett.* **108**, 206808 (2012).
- ²⁵ D. Kochan, M. Gmitra, and J. Fabian, *Phys. Rev. Lett.* **112**, 116602 (2014).
- ²⁶ D. Soriano, D. V. Tuan, S. M.-M. Dubois, M. Gmitra, A. W. Cummings, D. Kochan, F. Ortmann, J.-C. Charlier, J. Fabian, and S. Roche, *2D Materials* **2**, 022002 (2015).
- ²⁷ D. Kochan, S. Irmer, M. Gmitra, and J. Fabian, *Phys. Rev. Lett.* **115**, 196601 (2015).
- ²⁸ S. Omar, M. Gurram, I. Vera-Marun, X. Zhang, E. Huisman, A. Kaverzin, B. Feringa, and B. van Wees, *Phys. Rev. B* **92**, 115442 (2015).
- ²⁹ M. R. Thomsen, M. M. Ervasti, A. Harju, and T. G. Pedersen, *Phys. Rev. B* **92**, 195408 (2015).
- ³⁰ J. Bundesmann, D. Kochan, F. Tkatschenko, J. Fabian, and K. Richter, *Phys. Rev. B* **92**, 081403 (2015).
- ³¹ S. Lara-Avila, S. Kubatkin, O. Kashuba, J. A. Folk, S. Lüscher, R. Yakimova, T. J. B. M. Janssen, A. Tzalenchuk, and V. Fal'ko, *Phys. Rev. Lett.* **115**, 106602 (2015).
- ³² C. Ertler, S. Konschuh, M. Gmitra, and J. Fabian, *Phys. Rev. B* **80**, 041405 (2009).
- ³³ D. Van Tuan, F. Ortmann, D. Soriano, S. Valenzuela, and S. Roche, *Nature Physics* **10**, 857 (2014).
- ³⁴ Y. Liu, G. Bian, T. Miller, and T.-C. Chiang, *Phys. Rev. Lett.* **107**, 166803 (2011).
- ³⁵ D. Pesin and A. H. MacDonald, *Nature Materials* **11**, 409416 (2012).
- ³⁶ U. Zuelicke, in *Optoelectronic and Microelectronic Materials Devices COMMAD* (2014) pp. 54–55.
- ³⁷ A. Rycerz, J. Tworzydło, and C. Beenakker, *Nature Physics* **3**, 172 (2007).
- ³⁸ P. San-Jose, E. Prada, E. McCann, and H. Schomerus, *Phys. Rev. Lett.* **102**, 247204 (2009).
- ³⁹ G. Tkachov and M. Hentschel, *Phys. Rev. B* **79**, 195422 (2009).
- ⁴⁰ C. Park, H. Yang, A. J. Mayne, G. Dujardin, S. Seo, Y. Kuk, J. Ihm, and G. Kim, **108**, 18622 (2011).
- ⁴¹ D. Gunlycke and C. T. White, *Phys. Rev. Lett.* **106**, 136806 (2011).
- ⁴² M. B. Lundberg and J. A. Folk, *Science* **346**, 422 (2014).
- ⁴³ E. I. Rashba, *Phys. Rev. B* **79**, 161409 (2009).
- ⁴⁴ M. H. D. Guimarães, P. J. Zomer, J. Ingla-Aynés, J. C. Brant, N. Tombros, and B. J. van Wees, *Phys. Rev. Lett.* **113**, 086602 (2014).
- ⁴⁵ D. Van Tuan, F. Ortmann, A. Cummings, D. Soriano, and S. Roche, *Scientific Reports* (2015).
- ⁴⁶ S. Irmer, T. Frank, S. Putz, M. Gmitra, D. Kochan, and J. Fabian, *Phys. Rev. B* **91**, 115141 (2015).
- ⁴⁷ M. Gmitra, S. Konschuh, C. Ertler, C. Ambrosch-Draxl,

- and J. Fabian, Phys. Rev. B **80**, 235431 (2009).
- ⁴⁸ C. R. Ast and I. Gierz, Phys. Rev. B **86**, 085105 (2012).
- ⁴⁹ S. Yuan, M. Rösner, A. Schulz, T. O. Wehling, and M. I. Katsnelson, Phys. Rev. Lett. **114**, 047403 (2015).
- ⁵⁰ S. Roche and D. Mayou, Phys. Rev. Lett. **79**, 2518 (1997).
- ⁵¹ S. Roche, Phys. Rev. B **59**, 2284 (1999).
- ⁵² M. I. Dyakonov and V. I. Perel, Soviet Physics Solid State **13**, 3023 (1972).
- ⁵³ D. Huertas-Hernando, F. Guinea, and A. Brataas, Phys. Rev. Lett. **103**, 146801 (2009).
- ⁵⁴ P. Zhang and M. W. Wu, New Journal of Physics **14**, 033015 (2012).
- ⁵⁵ L. Zhao, R. He, K. Rim, T. Schiros, K. Kim, G. C. Zhou, H. and, S. Chockalingam, C. Arguello, L. Palova, D. Nordlund, M. Hybertsen, D. Reichman, T. Heinz, P. Kim, A. Pinczuk, G. Flynn, and A. Pasupathy, Science **333**, 999 (2011).
- ⁵⁶ K. S. Mali, J. Greenwood, J. Adisoejoso, R. Phillipson, and S. De Feyter, Nanoscale **7**, 1566 (2015).
- ⁵⁷ M. Wojtaszek, I. J. Vera-Marun, T. Maassen, and B. J. van Wees, Phys. Rev. B **87**, 081402 (2013).
- ⁵⁸ A. G. Swartz, K. M. McCreary, W. Han, J. J. I. Wong, P. M. Odenthal, H. Wen, J.-R. Chen, R. K. Kawakami, Y. Hao, R. S. Ruoff, and J. Fabian, Journal of Vacuum Science and Technology B **31**, 105 (2013).
- ⁵⁹ X. Hong, S.-H. Cheng, C. Herding, and J. Zhu, Phys. Rev. B **83**, 085410 (2011).
- ⁶⁰ A. Avsar, J. Lee, G. Koon, and B. Özyilmaz, 2D Materials **2**, 044009 (2015).
- ⁶¹ J. O. Sofo, A. M. Suarez, G. Usaj, P. S. Cornaglia, A. D. Hernández-Nieves, and C. A. Balseiro, Phys. Rev. B **83**, 081411 (2011).
- ⁶² M. Guzman-Arellano, A. D. Hernandez-Nieves, C. A. Balseiro, and G. Usaj, Appl. Phys. Lett. **105**, 121606 (2014).
- ⁶³ R. M. Guzmán-Arellano, A. D. Hernández-Nieves, C. A. Balseiro, and G. Usaj, Phys. Rev. B **91**, 195408 (2015).
- ⁶⁴ L. H. Guessi, Y. Marques, R. S. Machado, K. Kristinsson, L. S. Ricco, I. A. Shelykh, M. S. Figueira, M. de Souza, and A. C. Seridonio, Phys. Rev. B **92**, 245107 (2015).
- ⁶⁵ X. Hong, K. Zou, B. Wang, S.-H. Cheng, and J. Zhu, Phys. Rev. Lett. **108**, 226602 (2012).